PTEP

Prog. Theor. Exp. Phys. **2015**, 021D01 (8 pages)
DOI: 10.1093/ptep/ptv002

Letter

Observation of the "$K^- pp$"-like structure in the $d(\pi^+, K^+)$ reaction at 1.69 GeV/c

Yudai Ichikawa[1,2], Tomofumi Nagae[1,*], Hiroyuki Fujioka[1], Hyoungchan Bhang[3], Stefania Bufalino[4], Hiroyuki Ekawa[1,2], Petr Evtoukhovitch[5], Alessandro Feliciello[4], Shoichi Hasegawa[2], Shuhei Hayakawa[6], Ryotaro Honda[7], Kenji Hosomi[2], Ken'ichi Imai[2], Shigeru Ishimoto[8], Changwoo Joo[3], Shunsuke Kanatsuki[1], Ryuta Kiuchi[2], Takeshi Koike[7], Harphool Kumawat[9], Yuki Matsumoto[7], Koji Miwa[7], Manabu Moritsu[10], Megumi Naruki[1], Masayuki Niiyama[1], Yuki Nozawa[1], Ryosuke Ota[6], Atsushi Sakaguchi[6], Hiroyuki Sako[2], Valentin Samoilov[5], Susumu Sato[2], Kotaro Shirotori[10], Hitoshi Sugimura[2], Shoji Suzuki[8], Toshiyuki Takahashi[8], Tomonori N. Takahashi[10], Hirokazu Tamura[7], Toshiyuki Tanaka[6], Kiyoshi Tanida[3], Atsushi O. Tokiyasu[10], Zviadi Tsamalaidze[5], Bidyut Roy[9], Mifuyu Ukai[7], Takeshi O. Yamamoto[7], and Seongbae Yang[3]

[1]*Department of Physics, Kyoto University, Kyoto 606-8502, Japan*
[2]*ASRC, Japan Atomic Energy Agency, Ibaraki 319-1195, Japan*
[3]*Department of Physics and Astronomy, Seoul National University, Seoul 151-747, Korea*
[4]*INFN, Istituto Nazionale di Fisica Nucleare, Sez. di Torino, I-10125 Torino, Italy*
[5]*Joint Institute for Nuclear Research, Dubna, Moscow Region 141980, Russia*
[6]*Department of Physics, Osaka University, Toyonaka 560-0043, Japan*
[7]*Department of Physics, Tohoku University, Sendai 980-8578, Japan*
[8]*High Energy Accelerator Research Organization (KEK), Tsukuba, 305-0801, Japan*
[9]*Nuclear Physics Division, Bhabha Atomic Research Centre, Mumbai, India*
[10]*Research Center for Nuclear Physics (RCNP), Osaka University, Osaka 567-0047, Japan*
*E-mail: nagae@scphys.kyoto-u.ac.jp

Received November 21, 2014; Revised December 19, 2014; Accepted December 22, 2014; Published February 23, 2015

We have observed a "$K^- pp$"-like structure in the $d(\pi^+, K^+)$ reaction at 1.69 GeV/c. In this reaction, a $\Lambda(1405)$ hyperon resonance is expected to be produced as a doorway to form $K^- pp$ through the $\Lambda^* p \to K^- pp$ process. However, most of the $\Lambda(1405)$ produced would escape from the deuteron without secondary reactions. Therefore, coincidence of high-momentum (>250 MeV/c) proton(s) at large emission angles ($39^\circ < \theta_{\rm lab.} < 122^\circ$) was requested to enhance the signal-to-background ratio. A broad enhancement in the proton coincidence spectra is observed around the missing mass of 2.27 GeV/c^2, which corresponds to the $K^- pp$ binding energy of 95 $^{+18}_{-17}$ (stat.) $^{+30}_{-21}$ (syst.) MeV and the width of 162 $^{+87}_{-45}$ (stat.) $^{+66}_{-78}$ (syst.) MeV.

Subject Index D33

1. *Introduction* Whether or not kaonic nuclei exist is a key issue in developing our understanding of the $\bar{K}N$ interaction in vacuum and in nuclear medium. Information on the $\bar{K}N$ interaction has been obtained by analyzing low-energy $\bar{K}N$ scattering data and kaonic-atom X-ray data [1,2].

The recent measurement of the energy shift and width on a kaonic-hydrogen X-ray at high precision by the SIDDHARTA group [3,4] has contributed a lot [5]. From the theoretical analyses using these results, it is well known that the $\bar{K}N$ interaction has a strong attraction in the isospin 0 channel, which suggests the possible existence of kaonic bound-state formations [6–8]. Among them, the K^-pp bound state composed of a K^- and two protons could be the simplest one, if it existed.

Since this is a three-body system, several groups (see the recent summary in Ref. [9], particularly Table 1, and Refs. [10–12]) have calculated the binding energy and width of K^-pp by applying various few-body calculation techniques, such as variational and Faddeev-type calculations. The obtained binding energies are scattered over a broad range: 10–20 MeV for shallow potential cases and 50–100 MeV for deep cases. The width would be as wide as 70 MeV because of the strong $\bar{K}N$–$\pi\Sigma$ coupling. In addition, there could be non-mesonic absorption contributions of $\bar{K}NN \to \Lambda(\Sigma)N$.

The first experimental evidence of the K^-pp bound state was reported by the FINUDA collaboration [13] in the stopped K^- absorption reactions on ^{6}Li, ^{7}Li, and ^{12}C targets. They observed a lot of Λp pairs emitted back-to-back, and found the invariant mass of the pair to be significantly lower than the K^-pp mass threshold. A binding energy of $115\ ^{+6}_{-5}$ (stat.) $^{+3}_{-4}$ (syst.) MeV and a decay width of $\Gamma = 67\ ^{+14}_{-11}$ (stat.) $^{+2}_{-3}$ (syst.) MeV were obtained. However, there was a theoretical criticism [14–16] of the interpretation of the observed structure as a K^-pp bound state.

Another piece of experimental evidence was reported by the DISTO collaboration [17]. They measured the missing-mass and invariant-mass spectra in an exclusive reaction of $pp \to K^+\Lambda p$ at 2.85 GeV. A binding energy of 103 ± 3(stat.) ± 5(syst.) MeV and a width of 118 ± 8(stat.) $\pm$ 10(syst.) MeV were obtained. However, they did not observe the signal at 2.50 GeV [18], maybe due to the lower production cross section of $\Lambda(1405)$ at this energy.

There is also a report of a narrow and much deeper binding for the K^-pp system observed in $\bar{p}$–^{4}He annihilations at rest [19,20]. No peak was observed in the inclusive spectrum of the $\gamma d \to K^+\pi^-X$ reaction at $E_\gamma = 1.5$–2.4 GeV [21].

Thus, the experimental situation for the K^-pp bound state is not conclusive at this moment. It is important to obtain new experimental information in different reactions. In the J-PARC E27 experiment, we used the $d(\pi^+, K^+)$ reaction at 1.69 GeV/c to produce the K^-pp system, using the $\Lambda(1405)$ production as a doorway [22]. This is a simple production measurement with the smallest final-state effects.

2. *Experimental setup*

The experiment was carried out at the K1.8 beam line [23] of the hadron experimental hall at J-PARC [24]. In this beam line, separated $K^\pm$, $\pi^\pm$, p, and $\bar{p}$ beams up to 2 GeV/c are delivered. The details of the experimental setup for this measurement are described in Refs. [25,26].

The beam line is equipped with a beam line spectrometer for the incident π^+ momentum reconstruction, composed of four quadrupole magnets and one dipole magnet. The outgoing K^+ momentum was reconstructed with the superconducting kaon spectrometer (SKS) with a momentum resolution of $\Delta p/p \sim 2 \times 10^{-3}$.

A liquid hydrogen/deuterium target was installed 1.3 m upstream of the entrance of the SKS magnet, so that the solid angle acceptance of the SKS was about 100 msr. The size of the target cell was 120 mm in length and 67.3 mm in diameter, containing 1.99 g/cm^2 of liquid deuterium.

2.1 *Range counter arrays*

In order to suppress the large backgrounds coming from quasi-free productions of hyperons (Λ and Σ) and hyperon resonances ($\Lambda(1405)$ and $\Sigma(1385)$), a range counter

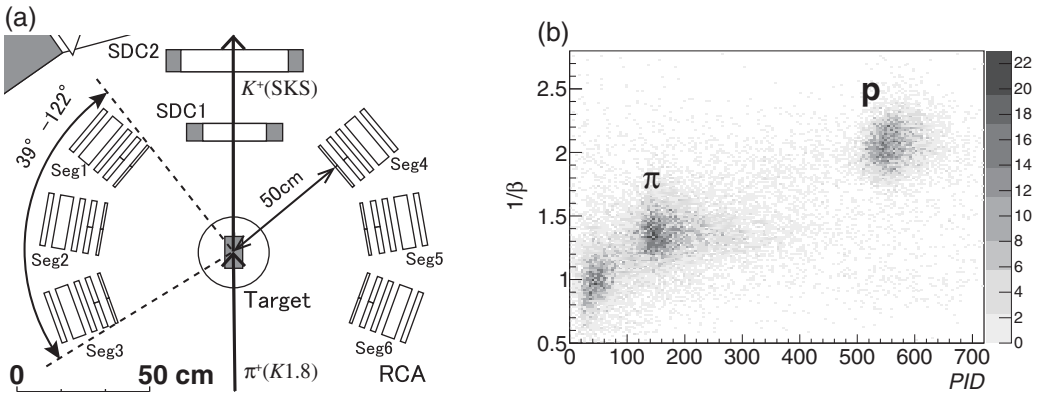

Fig. 1. (a) Schematic view of the range counter system. It was composed of six range counter arrays; three on the left (Seg1 to Seg3) and three on the right (Seg4 to Seg6) of the beam axis. SDC1 and 2 were the tracking drift chambers at the entrance of the SKS. (b) A scatter plot between the PID parameter and $1/\beta$. Protons are clearly separated from pions.

system was installed surrounding the liquid deuterium target at laboratory angles between 39° and 122°, on both the left and right sides from the beam axis, as shown in Fig. 1(a). The typical momentum of the produced system around the missing mass $MM_d \sim 2.27\,\mathrm{GeV}/c^2$ is about $0.6\,\mathrm{GeV}/c$ at the scattering angle $\theta_{\pi K} \sim 0°$ and we have a large acceptance to detect charged decay particles. We had three range counter arrays (RCAs) on each side and the assignment of the segment number is also shown in Fig. 1(a).

Each range counter array had five layers of plastic scintillation counters; the thickness of each scintillator was 1 cm, 2 cm, 2 cm, 5 cm, and 2 cm, respectively, with a height of 100 cm. The width of each layer was 20 cm. The first two layers were segmented into two slabs; each slab had 10 cm width. Therefore, we had seven $(2 + 2 + 1 + 1 + 1)$ scintillation counters in one range counter array. Every scintillation counter was read out from both sides (up and down) by photo-multiplier tubes (PMTs).

From each PMT, both hit timing and pulse height information were obtained. The discriminator threshold for the timing information was set at less than the one-tenth level of the minimum ionizing particles. The timing information from the first layer was used for the on-line trigger and the time-of-flight analysis off-line. The distance from the liquid target center to the first layer was about 50 cm. In the on-line trigger, the (π, K) trigger in coincidence with range counter hits was generated by requiring at least one hit among the 12 first-layer scintillators.

From a hit pattern of five layers, we can define the stopping layer, i_{stop}, for each range counter array. Then, we set up a particle identification parameter, PID, as,

$$PID = (dE_{i_{\mathrm{stop}}} + dE_{(i_{\mathrm{stop}}-1)})^{\alpha} - (dE_{i_{\mathrm{stop}}})^{\alpha}, \tag{1}$$

where dE_i shows the energy deposit in the ith layer of the plastic scintillators. The PID is a function of particle mass when the parameter $\alpha(\sim 1.75)$ is properly adjusted.

The time-of-flight (TOF) of each particle was obtained with the hit timing in the first layer. The flight path length was measured from the vertex position of the (π^+, K^+) reaction to the hit position on the first layer. In this analysis, the horizontal hit position was assumed to be the center of the scintillators and the vertical hit position was obtained from the time difference between the up and down PMTs. Then, the velocity of the particle (β) was obtained as $\beta = (\text{path length})/(\text{TOF} \cdot c)$, which was adjusted by using the π^+ produced from the $\Sigma^+ \to \pi^+ n$ decay in the $\pi^+ d \to K^+ \Sigma^+ X$ reaction.

Thus, we used the PID parameter and the velocity (β) for the particle identification between proton and pion. Figure 1(b) shows an example of a scatter plot between PID and $1/\beta$ in the case of $i_{\rm stop} = 4$ in one of the RCAs. In this analysis, the proton was selected as the gate of $\pm 3\sigma$ in PID and $\pm 2\sigma$ in $1/\beta$ for each stopping layer. Protons are clearly separated from pions. The energy of the proton was determined from the velocity.

From a study of the hydrogen target data, we could identify the proton from the Σ^+ decay ($\Sigma^+ \to p\pi^0$) with a detection efficiency of 65% for protons hitting the first layer of the RCA. The detection efficiency was limited due to leakage of particles at the side edges of the RCA. The systematic error of the detection efficiency might be overestimated by 20% at most, from our Monte Carlo simulations.

3. *Inclusive and coincidence analyses* Figure 2(a) shows the inclusive missing-mass (MM_d) spectrum for the $\pi^+ d \to K^+ X$ reaction at 1.69 GeV/c at scattering angles between 2° and 14° in the laboratory frame, which is a spectrum without acceptance correction. The overall missing-mass resolution was estimated from the missing-mass spectra of $\pi^+ p \to K^+ \Sigma^+$ reactions at 1.58 GeV/c and 1.69 GeV/c, and it was 2.8 ± 0.1 MeV/c^2 (FWHM). The details of the inclusive analyses were reported in Ref. [26].

As shown in Fig. 2(a), the missing-mass spectrum is composed of three major components: (I) the quasi-free $\pi^+ n \to K^+ \Lambda$ contribution (QFΛ), (II) the quasi-free $\pi^+ p \to K^+ \Sigma^+$ and $\pi^+ n \to K^+ \Sigma^0$ contributions (QFΣ), and (III) a mixture of the quasi-free $\pi^+ N \to K^+ \Sigma(1385)$, $\pi^+ n \to K^+ \Lambda(1405)$ (QFY^*), and $\pi^+ N \to K^+ (\Lambda/\Sigma)\pi$ (QF$Y\pi$). Between the QFΛ and QFΣ, we have a small peculiar structure corresponding to a threshold cusp for the $\Sigma N \to \Lambda N$ conversion process [26].

Next, we request the coincidence of one proton. According to our detector simulation, a proton emitted from the QFΛ, QFΣ, QFY^*, and QF$Y\pi$ processes rarely hits the RCA; only a small fraction in the very forward segments (Seg1, 4) does. The spectator proton in a deuteron rarely exceeds an analysis threshold momentum of 250 MeV/c. Therefore, we can expect good suppression of the quasi-free processes in the one-proton coincidence spectrum.

Figure 2(b) shows a coincidence spectrum with one proton in the middle segments of the RCA on each side (Seg2, 5). These segments have an almost flat and wide acceptance in missing mass, while the backward segments (Seg3, 6) have a limited acceptance for $K^- pp$. Note that there would be no quasi-free contributions in this spectrum according to the simulation. Possible non-quasi-free contributions are the $K^- pp$ signal emitting through $K^- pp \to \Lambda(\Sigma^0)p$, the threshold cusp background emitting through a strong conversion of $\Sigma^+ n \to \Lambda p$, and backgrounds of quasi-free hyperons and hyperon resonance productions followed by conversions such as $\Sigma N \to \Lambda N$.

In Fig. 2(c), we present a ratio histogram between the one-proton coincidence spectrum (Fig. 2(b)) and the inclusive one (Fig. 2(a)). This is a spectrum without acceptance correction for the RCA. The vertical axis shows the proton coincidence probability as a function of the missing mass. The contamination from the misidentification of $\pi^{+/-}$ in the RCA, which is estimated by the side-band events in PID, is shown by hatched spectra in Figs. 2(b) and (c). The contamination fraction of this component is about 7% around $MM_d \sim 2.27$ GeV/c^2.

We notice that there are two prominent structures: one at the threshold cusp position (2.13 GeV/c^2) and a broad bump at around 2.27 GeV/c^2, which could be a signal of the "$K^- pp$"-like structure. In the QFΣ and QFY^* regions, the proton coincidence probability is smaller than the two prominent structures and stays rather constant.

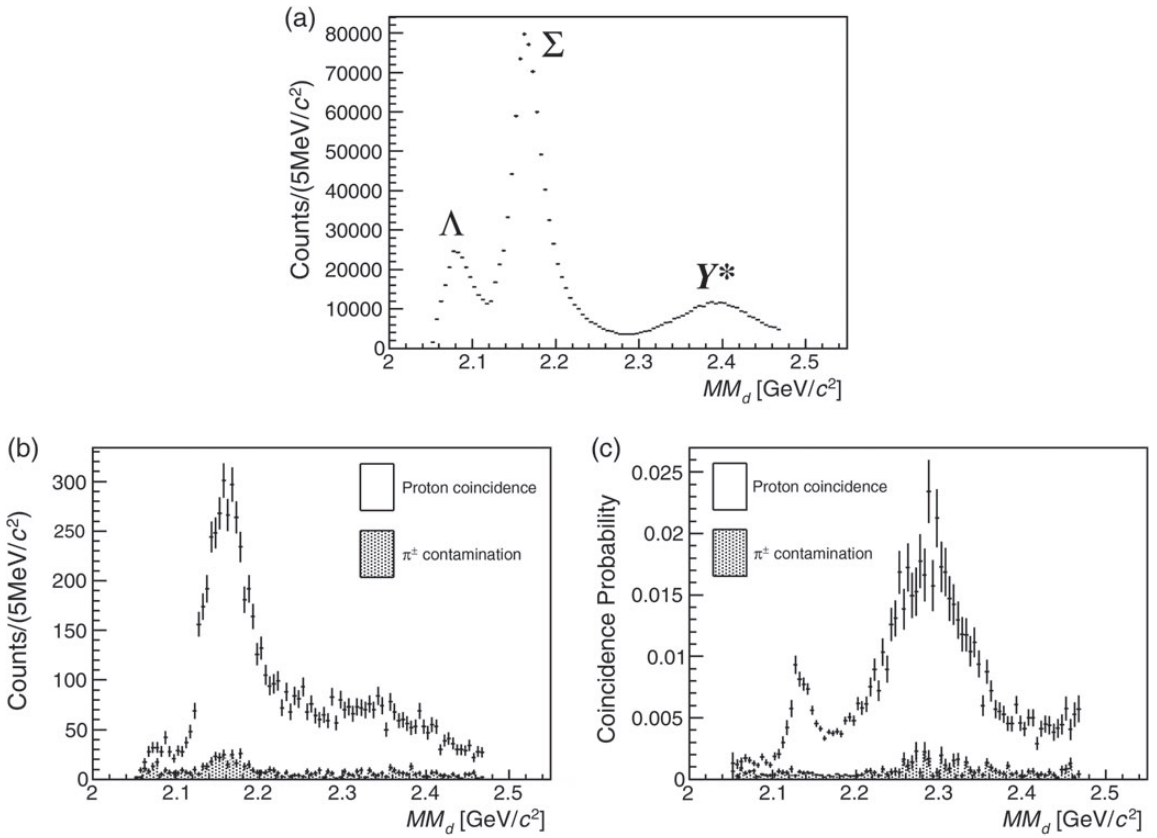

Fig. 2. (a) Inclusive missing-mass spectrum of the $d(\pi^+, K^+)$ reaction at 1.69 GeV/c at laboratory scattering angles from 2° to 14°. (b) Missing-mass spectrum of the $d(\pi^+, K^+)$ reaction with one proton in the middle of the RCA on each side (Seg2, 5). (c) The coincidence probability of a proton obtained by dividing the coincidence spectrum (b) with the inclusive spectrum (a). Hatched spectra show the contamination from the misidentification of $\pi^\pm$ in the RCA.

At this stage, the acceptance of our range counter system is not taken into account. The acceptance correction needs information on the decay modes of the "$K^- pp$"-like structure. This study was carried out by requiring coincidence of two protons in the RCAs. All possible combinations of two segments were used in this analysis; the combination of Seg1 and 4 gives the largest yield. In such a condition, we can measure the missing mass of X in the $d(\pi^+, K^+ pp)X$ process by detecting two protons in the decay of the ppX system, the mass of which is MM_d, in three categories: (i) Λp, $\Lambda \to p\pi^-$, (ii) $\Sigma^0 p$, $\Sigma^0 \to \Lambda\gamma \to p\pi^-\gamma$, and (iii) $Y\pi\mathrm{N} \to pp\pi\pi$. The first two modes, (i) and (ii), are non-mesonic and the X is one pion (and γ). The last one, (iii), is mesonic and the X is two pions. Therefore, the missing-mass spectrum of M_X should show different distributions for each decay mode. Figure 3 shows such missing-mass square spectra for M_X. Three distributions estimated for each decay mode are shown in the figure by fitting the height of each template distribution. These templates were made from the simulation, which assumes the reaction of $\pi^+ d \to K^+ W$, $W \to pY(p(Y\pi))$ with uniform productions and decays in the center-of-mass system. The probability of each final state has been estimated from the fitting of M_X^2 spectra.

Thus, we can correct the missing-mass spectrum with the acceptance of the RCAs, which depends on the decay mode. Each event is given a weight, equal to the probability of belonging to a specific decay mode, as a function of MM_d and M_X^2. The RCA acceptance is almost smooth in the missing mass except near the threshold of each decay mode. Figure 4(a) shows a missing-mass distribution for

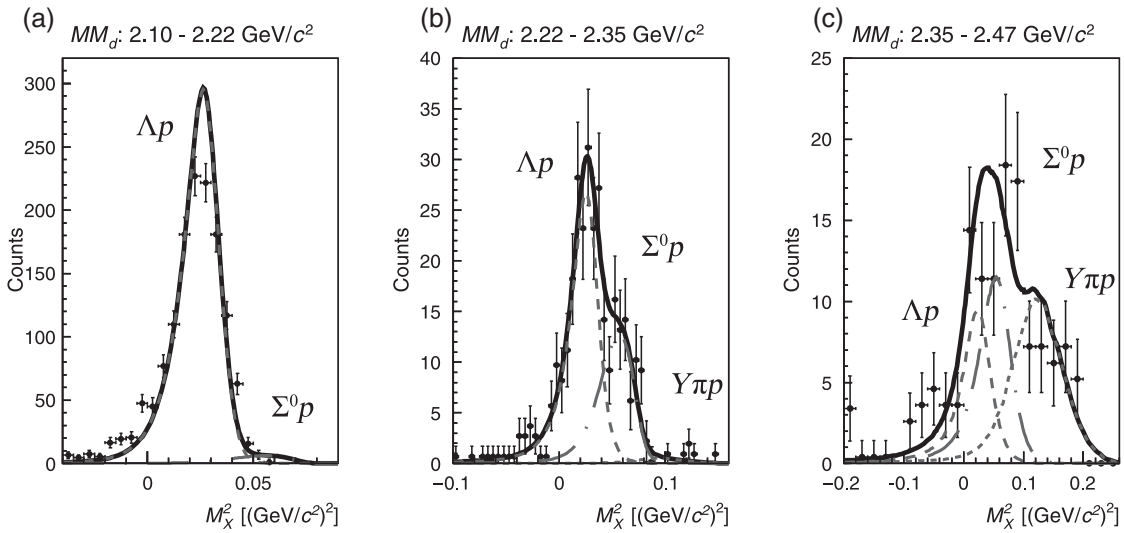

Fig. 3. Missing-mass square spectra of X obtained in two-proton coincidence events in the $d(\pi^+, K^+pp)X$ reaction. Each spectrum shows the mass square of X for a different MM_d region: the left (a) shows the QFΣ region ($MM_d < 2.22\,\mathrm{GeV}/c^2$), the center (b) shows the "K^-pp"-like structure region ($2.22 < MM_d < 2.35\,\mathrm{GeV}/c^2$), and the right (c) shows the QFY^* region ($MM_d > 2.35\,\mathrm{GeV}/c^2$). The spectra were fitted with three components of Λp (dashed line), $\Sigma^0 p$ (dot-dashed line), and $Y\pi p$ (dotted line) decay modes.

two-proton coincidence events of the $\Sigma^0 p$ final state (ii) with the acceptance correction. According to the simulation, the contribution of the $\Sigma^0 p \to \Sigma^0 p$ rescattering background is negligible because of the two high-momentum proton coincidence. The spectrum was fitted with a relativistic Breit–Wigner function:

$$f(MM_d) = \frac{(2/\pi)MM_d m_0 \Gamma(q)}{(m_0^2 - MM_d^2)^2 + (m_0\Gamma(q))^2}. \tag{2}$$

The mass-dependent width was $\Gamma(q) = \Gamma_0(q/q_0)$, in which q (q_0) is the momentum of the Σ^0 and proton in the $\Sigma^0 p$ rest frame at mass MM_d (m_0). The obtained mass and width are $2275\ ^{+17}_{-18}$ (stat.) $^{+21}_{-30}$ (syst.) MeV/c^2 and $162\ ^{+87}_{-45}$ (stat.) $^{+66}_{-78}$ (syst.) MeV, respectively. This corresponds to the binding energy of the K^-pp system of $95\ ^{+18}_{-17}$ (stat.) $^{+30}_{-21}$ (syst.) MeV and the production cross section of the "K^-pp"-like structure decaying to $\Sigma^0 p$ of $d\sigma/d\Omega_{K^-pp\to\Sigma^0 p} = 3.0 \pm 0.3$ (stat.) $^{+0.7}_{-1.1}$ (syst.) μb/sr. The systematic errors of these values were estimated taking into account uncertainties in the fitting ranges, the binning of the missing-mass spectrum, the detection efficiency of two protons in the RCA, and the Breit–Wigner shape by changing the Lorentzian function folded with the missing-mass resolution. The differential cross section of the "K^-pp"-like structure of the Λp decay mode (i) was also estimated from the fitting assuming the same distribution of MM_d. Thus, a branching fraction of the "K^-pp"-like structure was obtained as $\Gamma_{\Lambda p}/\Gamma_{\Sigma^0 p} = 0.92\ ^{+0.16}_{-0.14}$ (stat.) $^{+0.60}_{-0.42}$ (syst.). This ratio was discussed from a theoretical point of view and predicted to be 1.2 using the chiral unitary model in Ref. [27].

Next, we try to understand the ratio histogram (Fig. 2(c)) with the obtained K^-pp mass distribution of $f(MM_d)$. By using the mass distribution for the "K^-pp"-like structure and the double-differential cross section of the inclusive (π^+, K^+) process $\frac{d^2\sigma}{d\Omega dMM_d}(MM_d)_{\mathrm{inclusive}}$, we can obtain the ratio

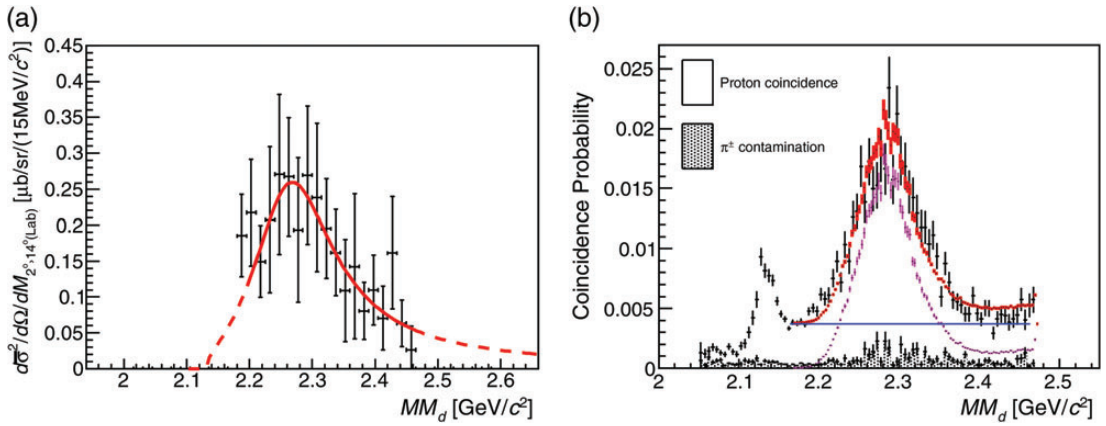

Fig. 4. (a) Missing-mass spectrum of the $d(\pi^+, K^+)$ reaction for two-proton coincidence and the $\Sigma^0 p$ decay branch events. The mass acceptances of the RCAs are corrected. The spectrum was fitted with a relativistic Breit–Wigner function (see text for details). We found a mass 2275 $^{+17}_{-18}$ (stat.) $^{+21}_{-30}$ (syst.) MeV/c^2 and a width 162 $^{+87}_{-45}$ (stat.) $^{+66}_{-78}$ (syst.) MeV. (b) The coincidence probability of one proton for the middle segment of the RCA, as in Fig. 2(c), together with the interpretation spectra shown as a colored line. See text for details.

histogram, shown in Fig. 4(b) as a plot colored in pink, which is calculated as

$$R_p(MM_d) = \frac{C \times f(MM_d) \times \eta_{1p}(MM_d)}{(\frac{d^2\sigma}{d\Omega dMM_d}(MM_d))_{\text{inclusive}}}, \tag{3}$$

where C is the normalization constant, and $\eta_{1p}(MM_d)$ is the detection efficiency of a proton in the middle segments of the RCA (Seg2, 5). The blue line in Fig. 4(b) is an assumed flat component representing the conversion processes and the contamination from the misidentification of $\pi^\pm$ in the RCA. Red points with error bars in Fig. 4(b) are the sum of the pink points and blue line. The normalization constant C and the amplitude of the flat component (blue line) were adjusted to minimize the differences between the black and red points. Thus, the obtained one-proton coincidence probability spectrum of the broad enhanced region could be reproduced by the "$K^- pp$" signal and flat background.

What is the nature of the "$K^- pp$"-like structure? It should have strangeness -1 and baryon number $B = 2$ from the observed reaction mode, so that the hyper charge $Y = 1$. As for the spin of the $K^- pp$ system, a K^- is theoretically assumed to couple with a spin-singlet ($S = 0$) p–p pair in an S-wave ($L = 0$), so that the $J^P = 0^-$, presumably. An alternative view of the system as a $\Lambda^* p$ bound state [28] also predicts the bound-state spin to be 0. There is also a theoretical prediction of a $(Y, I, J^P) = (1, 3/2, 2^+)$ dibaryon as a $\pi\Lambda N$–$\pi\Sigma N$ bound state [29].

4. *Summary* We have observed a "$K^- pp$"-like structure in the $d(\pi^+, K^+)$ reaction at 1.69 GeV/c with coincidence of high-momentum (>250 MeV/c) proton(s) at large emission angles ($39^\circ < \theta_{\text{lab.}} < 122^\circ$). A broad enhancement in the proton coincidence spectra is observed around the missing mass of 2.27 GeV/c^2, which corresponds to a binding energy of the $K^- pp$ system of 95 $^{+18}_{-17}$ (stat.) $^{+30}_{-21}$ (syst.) MeV and a width of 162 $^{+87}_{-45}$ (stat.) $^{+66}_{-78}$ (syst.) MeV. The branching fraction between the Λp and $\Sigma^0 p$ decay modes of the "$K^- pp$"-like structure was measured for the first time as $\Gamma_{\Lambda p}/\Gamma_{\Sigma^0 p} = 0.92\ ^{+0.16}_{-0.14}$ (stat.) $^{+0.60}_{-0.42}$ (syst.).

Acknowledgements

We would like to thank the Hadron beam channel group, accelerator group, and cryogenics section at J-PARC for their great efforts with stable machine operation and beam quality improvements. The authors are grateful for the support of NII for SINET4. This work was supported by a Grant-In-Aid for Scientific Research on Priority Area No. 449 (No. 17070005), a Grant-In-Aid for Scientific Research on Innovative Area No. 2104 (No. 22105506), from the Ministry of Education, Culture, Sports, Science and Technology (MEXT) Japan, and Basic Research (Young Researcher) No. 2010-0004752 from the National Research Foundation in Korea. We are grateful for the support of the National Research Foundation, WCU program of the Ministry of Education, Science and Technology (Korea), Center for Korean J-PARC Users.

References

[1] A. D. Martin, Nucl. Phys. B **179**, 33 (1981).
[2] N. Kaiser, P. B. Siegel, and W. Weise, Nucl. Phys. A **594**, 325 (1995).
[3] M. Bazzi et al., Phys. Lett. B **704**, 113 (2011).
[4] M. Bazzi et al., Nucl. Phys. A **881**, 88 (2012).
[5] T. Hyodo, Nucl. Phys. A **914**, 260 (2013).
[6] Y. Akaishi and T. Yamazaki, Phys. Rev. C **65**, 044005 (2002).
[7] T. Yamazaki and Y. Akaishi, Phys. Lett. B **535**, 70 (2002).
[8] T. Kishimoto, Phys. Rev. Lett. **83**, 4701 (1999).
[9] A. Gal, Nucl. Phys. A **914**, 270 (2013).
[10] S. Maeda, Y. Akaishi, and T. Yamazaki, Proc. Jpn. Acad. B **89**, 418 (2013).
[11] M. Bayar and E. Oset, Phys. Rev. C **88**, 044003 (2013).
[12] J. Révai and N. V. Shevchenko, Phys. Rev. C **90**, 034004 (2014).
[13] M. Agnello et al., Phys. Rev. Lett. **94**, 212303 (2005).
[14] V. K. Magas, E. Oset, A. Ramos, and H. Toki, Phys. Rev. C **74**, 025206 (2006).
[15] A. Ramos, V. K. Magas, E. Oset, and H. Toki, Nucl. Phys. A **804**, 219 (2008).
[16] V. K. Magas, E. Oset, and A. Ramos, Phys. Rev. C **77**, 065210 (2008).
[17] T. Yamazaki et al., Phys. Rev. Lett. **104**, 132502 (2010).
[18] P. Kienle et al., Eur. Phys. J. A **48**, 183 (2012).
[19] G. Bendiscioli et al., Eur. Phys. J. A **40**, 11 (2009).
[20] G. Bendiscioli et al., Nucl. Phys. A **789**, 222 (2007).
[21] A. O. Tokiyasu et al., Phys. Lett. B **728**, 616 (2014).
[22] T. Yamazaki and Y. Akaishi, Phys. Rev. C **76**, 045201 (2007).
[23] T. Takahashi et al., Prog. Theor. Exp. Phys. **2012**, 02B010 (2012).
[24] S. Nagamiya, Prog. Theor. Exp. Phys. **2012**, 02B001 (2012).
[25] Y. Ichikawa et al., presentation at "The 2nd International Symposium on Science at J-PARC 2014", Tsukuba July 2014. The proceedings will be published in JPS Conference Proceedings.
[26] Y. Ichikawa et al., Prog. Theor. Exp. Phys. **2014**, 101D03 (2014).
[27] T. Sekihara, D. Jido, and Y. Kanada-En'yo, Phys. Rev. C **79**, 062201(R) (2009).
[28] T. Uchino, T. Hyodo, and M. Oka, Nucl. Phys. A **868**, 53 (2011).
[29] H. Garcilazo and A. Gal, Nucl. Phys. A **897**, 167 (2013).